

COMPUTING ANGULARLY-RESOLVED FAR-FIELD EMISSION SPECTRA IN PARTICLE-IN-CELL CODES USING GPUS

R. Pausch^{†*}, H. Burau[†], M. Bussmann, J. Couperus, T. Cowan[†], A. Debus, A. Huebl[†], A. Irman, A. Köhler[†], U. Schramm[†], K. Steiniger[†], R. Widera
Helmholtz-Zentrum Dresden - Rossendorf (HZDR), 01314 Dresden
[†](also associated with: Technische Universität Dresden, 01062 Dresden)

Abstract

We present a self-consistent method to compute angularly resolved far-field spectra for both coherent and incoherent radiation which enables unprecedented quantitative predictions by taking into account emissions from all $\sim 10^{10}$ electrons simulated in PIC codes for hundreds to thousands of directions and frequencies. This is applied to predicting the radiation flux seen in plasma-based light sources or as synthetic diagnostics in laser-driven accelerators. We present simulated spectra from laser wakefield acceleration and examine the implementation and scalability of our many-GPU simulation code.

INTRODUCTION

Computing the radiation emitted from accelerated electrons in plasmas is of interest for both predicting angular resolved intensities of plasma based light sources and as synthetic diagnostics of the fs - nm scale electron dynamics in the plasma, which are not directly accessible to observation in experiments. Although the full electron and ion dynamics in a plasma is simulated self-consistently using particle-in-cell (PIC) codes [1, 2], deriving the spectrally and angularly resolved far-field radiation from the particle trajectories provided by PIC codes is challenging because the number of particles to track, as well as the number of directions and frequencies to resolve is high. In order to avoid these issues, some PIC simulations compute the emitted far-field radiation without angular resolution and consider a limited number of electrons $N_e < 10^6$ [3–6] or resolve the radiation angularly with up to $N_{\vec{n}} \leq 1000$ observation angles for only $N_e < 10^2$ particles [7, 8]. Currently, only PConGPU is capable of computing angularly resolved far-field radiation spectra for all billions of particles simulated [9].

When both coherent and incoherent radiation are present it is essential to take into account all particles. The emitted intensity from coherently radiating electrons scales quadratically with the number of particles $\sim N_e^2$, while the intensity of incoherently radiating electrons scales linearly $\sim N_e$. Thus for correct absolute emitted intensities, accurate ratios between coherent and incoherent contributions and realistic magnitudes of quasi-random noise, it is necessary to evaluate the spectra from all particle trajectories in the simulation, which ideally matches the real number of physical electrons. On the inter-particle level this is done by computing the relativistic time retardation of the radiation, i.e. the summed

up relative phase with respect to a target wavelength and observation direction, between all simulated particles. At the level of each individual macro-particle the degree of coherence of a given radiation wavelength is approximated by assuming a form factor [9], while neglecting any macro-particle substructures. Since such simulation results mimic experimental measurements and are acquired online during simulation, these are thus dubbed *synthetic diagnostics*.

ANGULARLY RESOLVED FAR-FIELD RADIATION SPECTRA

Accelerated charged particles emit electromagnetic radiation that can be detected far away from the particles. For any observation direction, the spectrally resolved far-field radiation can be calculated using Eq. 1, which is based on Liénard-Wiechert potentials [10].

$$\frac{d^2 I}{d\Omega d\omega}(\omega, \vec{n}) = \frac{1}{16\pi^2 \epsilon_0 c} \cdot |\vec{A}(\omega, \vec{n})|^2 \quad (1)$$

$$\vec{A} = \sum_{k=1}^{N_e} \int_{-\infty}^{+\infty} dt q_k \frac{\vec{n} \times [(\vec{n} - \vec{\beta}_k) \times \dot{\vec{\beta}}_k]}{(1 - \vec{\beta}_k \cdot \vec{n})^2} e^{i\omega(t - \vec{n}\vec{r}_k/c)} \quad (2)$$

Here, we sum over all N_e particles simulated, with q_k , \vec{r}_k , $\vec{\beta}_k$, $\dot{\vec{\beta}}_k$ being the charge, location, velocity and acceleration of particle k respectively as depicted in Fig. 1. The variables

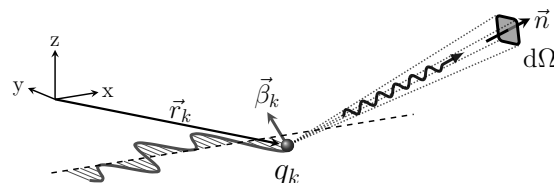


Figure 1: Radiation of the k^{th} electron at position \vec{r}_k , charge q_k and velocity $\vec{\beta}_k$ emitted towards the direction \vec{n} .

ϵ_0 , t and c represent vacuum permittivity, time and speed of light. The spectrally and angularly resolved emitted intensity $\frac{d^2 I}{d\Omega d\omega}$ depends on the frequency ω and the observation direction defined by the unit vector \vec{n} . The complex amplitudes \vec{A} , given in Eq. 2, correspond to a Fourier transform of the particle trajectories over the retarded time $t_{\text{ret}} = t - \vec{n}\vec{r}_k/c$. These vector amplitudes thus contain information on the polarization and phase of the emitted radiation and can be

* r.pausch@hzdr.de

used to reconstruct the complete dynamics of the particle phase space.

Note, that equation 1 is valid if the radiation can be considered to be purely classical and the emitted energy of a single particle is small compared to its kinetic energy $E_{\text{rad}} \ll E_{\text{kin}} = (\gamma - 1)m_e c^2$.

RADIATION FROM LASER WAKEFIELD ACCELERATION

The brilliance of Laser-wakefield accelerator (LWFA) light sources, such as synchrotron radiation in the X-ray range from betatron oscillation, directly depends on the phase space density of the radiating electrons within the plasma wave. Our PIConGPU code can calculate both the angularly resolved, absolute photon fluxes of these light sources and the detailed radiation signatures arising from the plasma dynamics, which determine electron beam formation and hence the brilliance of the plasma-based light source. In Laser-wakefield accelerators, the electron injection process and the subsequent acceleration within the plasma cavity are both critical for providing and maintaining high phase-space densities in the resulting electron beams. The highly non-linear nature of electron injection and acceleration makes it thus vital to accurately measure and control the laser-plasma dynamics in order to optimize the brilliance of LWFA light sources. This connection between measured radiation signatures, the associated plasma dynamics and the resulting X-ray spectra is provided by our code.

Due to the (sub-)micrometer spatial scales of plasma structures and electron bunches in laser wakefield accelerator, the emitted radiation exhibits a rich mixture of coherent and incoherent radiation, so that a full treatment of coherence in the emitted plasma radiation is necessary.

In order to demonstrate the capability of PIConGPU to predict absolute intensity values in this partially-coherent regime, we simulated a toy-model LWFA scenario (Fig. 2). The emitted radiation is simulated for a 800 μm , Gaussian laser pulse with pulse length $\tau = 10$ fs and normalized laser strength $a_0 = 2.0$, which drives a bubble in a plasma with an initial electron density of $n_e = 2.5 \cdot 10^{18} \text{cm}^{-3}$. The intensity spectrum in Fig. 2 shows the total emitted radiation spectrum of the laser-plasma interaction 290 fs after the laser has entered the plasma.

Although the harmonics structure of the spectrum resembles the general spectrum of a Thomson-scattered laser within a plasma, the plasma dynamics of LWFA leads to intensities and angular distributions that are distinctly different from those predicted by analytical models [11], which do not consider the LWFA plasma dynamics. These differences are encoded in the harmonics width, the angular distribution, as well as the harmonics relative peak intensity ratios or intensity contrast with respect to the background. Since the differences are based on the structure and dynamics of the plasma, these become relevant for any attempt of deducing the LWFA properties from experimentally obtained plasma

self-emission spectra, which are usually intensity spectra without direct phase information.

Hence these radiation simulations make it now possible to quantitatively examine experimental spectral data, which on the one hand is easily available, but on the other hand hard to analyze, since the complexity of laser-plasma interactions makes it exceedingly difficult to connect spectral signatures to plasma dynamics. Once the spectral features most sensitive to the plasma structure and dynamics are identified, the experimental spectra can be used to directly optimize and control LWFA-based light sources, such as from betatron oscillations, without referring to the simulation.

IMPLEMENTATION OF THE SYNTHETIC RADIATION DIAGNOSTIC IN PICONGPU

Computing the far-field radiation using Eq. 1 is computationally challenging. Summing over $N_e \sim 10^{10}$ particles for each time step N_t requires to access particle data of ~ 100 TB. A high data transfer rate is therefore essential when computing the spectra. Computing the complex amplitudes requires a total of $N_t \cdot N_e \cdot N_\omega \cdot N_{\vec{n}}$ evaluations of the summand in Eq. 2, with N_ω being the number of frequencies and $N_{\vec{n}}$ being the number of observation directions computed. Typical numbers for these quantities are $N_e \sim 10^9$, $N_t \sim 10^5$, $N_\omega \sim 10^2$ and $N_{\vec{n}} \sim 10^2$ which results in $\sim 10^{18}$ evaluations in total. Thus, evaluating Eq. 1 requires a large number of floating point operations (FLOPs). As an example, for the simulation presented in [12] there were $9 \cdot 10^{18}$ evaluations of the summand. This is $\sim 10^8$ times more than performed by the simulation mentioned in the introduction [3], but was still completed in under one day.

With PIConGPU [13, 14], computing the particle dynamics and emitted radiation is done entirely on GPUs. This allows to read particle trajectory data for evaluating Eq. 1 directly from the GPU memory, where data transfer rates of 0.25 TB/s per GPU are available [15]. Compared to any bandwidth accessible when storing and post-processing trajectories on hard-drive, the memory bandwidth on GPUs is orders of magnitude larger. Additionally, compute rates of ~ 1.3 TFLOPs per GPU are available if the evaluation of Eq. 1 is distributed efficiently on the ~ 2500 ALUs of each GPU. This allows to perform the floating point operations required to solve Eq. 1 approximately one order of magnitude faster compared to performing it on CPU. Without both the high data transfer rates and the high compute rates available on GPUs, computing angularly-resolved far-field emission spectra would be impossible for all particles in a plasma simulation.

PROOF OF CONCEPT: EXASCALE RADIATION SIMULATION

PIConGPU is capable of computing the spectrally and angularly resolved far-field radiation of large-scale laser-plasma simulations as recently proven in performing a similar sized simulation of an astrophysical jet in which we

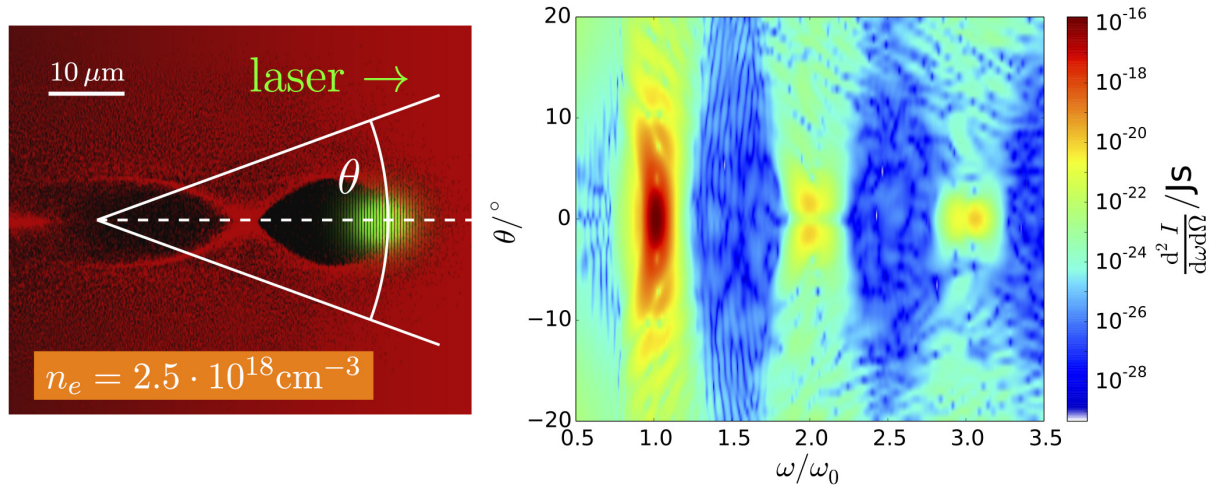


Figure 2: Left: The far-field observation angle θ shown in front of the density of the plasma drawn in red and the laser drawn in green. The background plasma has an electron density of $n_e = 2.5 \cdot 10^{18} \text{cm}^{-3}$ and the gaussian laser pulse has an peak intensity of $a_0 = 2.0$. Right: The emitted energy per unit frequency and unit solid angle $\frac{d^2 I}{d\omega d\Omega}$ is plotted over the emitted frequency ω in units of the laser frequency ω_0 and the observation angle θ (observation direction $\vec{n} = (\sin \theta, \cos \theta, 0)$, with x being the laser polarization direction and y the laser propagation direction). $N_e = 75 \cdot 10^6$ macro-particles were analyzed for $N_t = 6000$ time steps and the radiation was calculated for $N_\omega = 512$ frequencies and $N_{\vec{n}} = 64$ directions to generate the spectral plot.

computed the far-field radiation of the relativistic Kelvin-Helmholtz instability [12, 14]. This simulation was at the leading edge of what is possible with computer simulations today.

The astrophysical simulation covered 75 billion macro particles on 4.7 billion cells. The far-field radiation was computed on a quadrant of the sky map with $N_{\vec{n}} = 481$ observation directions and $N_\omega = 512$ frequency on a logarithmic scale using a non-equidistant discrete Fourier transform. On 18.432 GPUs the code reached a peak performance of 7.176 PFLOPs (double precision). A total of 1.34 PByte of particle data was read while evaluating the far-field radiation. Even with this large-scale simulation, PIConGPU performed with 96% weak efficiency. The total simulation time was 16 h for 2000 time steps.

Translating these performances to a LWFA simulation with $2048 \times 512 \times 512$ cells and $N_t = 30,000$ time steps and computing the radiation for a similar quadrant of the spectral sky map on 2000 GPUs would require 2.5 days of simulation time. Compared to the simulation of the Kelvin-Helmholtz instability, which ran on the world's second largest cluster, such a LWFA simulation can be performed on several powerful GPU clusters available today.

CONCLUSIONS

We have shown that for Laser-wakefield accelerator (LWFA) simulations our GPU-accelerated particle-in-cell code PIConGPU provides angularly resolved spectra based on all billions of particles during a PIC simulation including coherence and polarization properties. This full-scale ap-

proach of quantitatively simulating the far-field radiation in plasmas is unprecedented and enables a range of new optimization strategies for all plasma-based light sources. First results show that the product of frequencies and observation directions calculated in LWFA simulations typically reaches up to $\sim 10^6$ using existing HPC GPU clusters. The achieved performance makes it possible to extend our technique to calculate spectral images based on a million observation directions for a few selected wavelengths, as done in experiment by spectrally filtered CCD imaging, hence revealing the sources of plasma radiation.

REFERENCES

- [1] R.W. Hockney and J.W. Eastwood. *Computer simulation using particles*. Taylor & Francis, 1988.
- [2] John M Dawson. Particle simulation of plasmas. *Reviews of modern physics*, 55(2):403, 1983.
- [3] Lorenzo Sironi and Anatoly Spitkovsky. Synthetic spectra from particle-in-cell simulations of relativistic collisionless shocks. *The Astrophysical Journal Letters*, 707(1):L92, 2009.
- [4] Troels Haugboelle, Jacob Trier Fredriksen, and Aake Nordlund. Photon-Plasma: a modern high-order particle-in-cell code. *arXiv preprint arXiv:1211.4575*, 2012.
- [5] K-I Nishikawa, P Hardee, B Zhang, I Dutan, M Medvedev, EJ Choi, KW Min, J Niemiec, Y Mizuno, A Nordlund, et al. Radiation from accelerated particles in relativistic jets with shocks, shear-flow, and reconnection. *arXiv preprint arXiv:1303.2569*, 2013.
- [6] Christian Busk Hededal and Åke Nordlund. Gamma-ray burst synthetic spectra from collisionless shock PIC simulations. *arXiv preprint astro-ph/0511662*, 2005.

- [7] JL Martins, SF Martins, RA Fonseca, and LO Silva. Radiation post-processing in PIC codes. In *SPIE Europe Optics+ Optoelectronics*, pages 73590V–73590V. International Society for Optics and Photonics, 2009.
- [8] AGR Thomas. Algorithm for calculating spectral intensity due to charged particles in arbitrary motion. *Physical Review Special Topics-Accelerators and Beams*, 13(2):020702, 2010.
- [9] R. Pausch, A. Debus, R. Widera, K. Steiniger, A. Huebl, H. Burau, M. Bussmann, and U. Schramm. How to test and verify radiation diagnostics simulations within particle-in-cell frameworks. *Nuclear Instruments and Methods in Physics Research Section A: Accelerators, Spectrometers, Detectors and Associated Equipment*, 740(0):250–256, 2014. Proceedings of the first European Advanced Accelerator Concepts Workshop 2013.
- [10] J. D. Jackson. *Classical Electrodynamics*. John Wiley and Sons, Inc., 1999.
- [11] Eric Esarey, Sally K Ride, and Phillip Sprangle. Nonlinear Thomson scattering of intense laser pulses from beams and plasmas. *Physical Review E*, 48(4):3003, 1993.
- [12] Axel Huebl, David Pugmire, Felix Schmitt, Richard Pausch, and Michael Bussmann. Visualizing the Radiation of the Kelvin-Helmholtz Instability. *arXiv preprint arXiv:1404.2507*, 2014.
- [13] H. Burau, R. Widera, W. Hönig, G. Juckeland, A. Debus, T. Kluge, U. Schramm, T.E. Cowan, R. Sauerbrey, and M. Bussmann. PIConGPU: a fully relativistic particle-in-cell code for a GPU cluster. *Plasma Science, IEEE Transactions on*, 38(10):2831–2839, 2010.
- [14] M. Bussmann, H. Burau, T. E. Cowan, A. Debus, A. Huebl, G. Juckeland, T. Kluge, W. E. Nagel, R. Pausch, F. Schmitt, U. Schramm, J. Schuchart, and R. Widera. Radiative Signatures of the Relativistic Kelvin-Helmholtz Instability. In *Proceedings of the International Conference on High Performance Computing, Networking, Storage and Analysis, SC '13*, pages 5:1–5:12, New York, NY, USA, 2013. ACM.
- [15] NVIDIA Corporation. Tesla GPU accelerators for servers. <http://www.nvidia.com/object/tesla-servers.html>, June 2014.